

# DEVELOPMENT OF AN UNDERGROUND THROUGH-SOIL WIRELESS ACOUSTIC COMMUNICATION SYSTEM

Sijung Yang, Omar Baltaji, Andrew C. Singer, and Youssef M. A. Hashash

## ABSTRACT

The practical development of WUSN would benefit numerous applications, including online infrastructure monitoring, earthquake warning systems, and agricultural automation. However, state-of-the-art RF electromagnetic wireless systems are ineffective for communicating through-soil, due to extreme signal path losses from absorption and scattering in soil, even though the typical data requirements for such applications are modest, ranging from tens to hundreds of bps. In contrast, elephants, rodents and a wide variety of insects use acoustic waves for communicating through-soil, suggesting the viability of soil as a communication channel, and of acoustic waves as carriers. In this article, we demonstrate how soil can be used as a communication medium for wireless acoustic digital communication over distances up to 50 m at 20 bps data rates. By leveraging a physical model of the soil channel derived from its identified characteristics, then employing QPSK and OOK modulation and sparse decision feedback equalization schemes, and exploiting well-coupled and matched acoustic sources, wireless digital communication was successful in both laboratory and field experiments, illustrating the viability of sending application-specific data, ranging from binary sensor readings to low-resolution images.

## INTRODUCTION

Underground applications, such as mining, infrastructure construction, and agricultural monitoring, typically rely on numerous embedded sensors such as piezometers, accelerometers, extensometers, and others, to supply real-time vital measurements about soil properties, structural health, or seismic activity. These sensors are usually installed in small-diameter boreholes underground, where wires are extended from the sensors to the above-ground data loggers which can be accessed manually or remotely, via through-air wireless systems. With increased experience in manufacturing sensors, internal sensor failure has become less likely. However, the vulnerability of wires to damage due to ground deformations, construction activities, and biological and chemical underground hostility persists and shows the need for wireless networks for underground sensors. This issue is magnified when more than one sensor is deployed in a borehole, connected serially, making the sensor cluster no more robust than the weakest point in its connecting wires. Further-

more, the cost of wires commonly exceeds that of sensors, especially when they are deployed in deep earth [1].

For a wireless communication system to be suitable for such applications, it should be capable of transmitting data over few to tens of meters of soil. These applications typically require data rates on the order of tens of bits per day; from one to a few measurements per day is usually considered satisfactory, since the changes underground are typically slow. The energy efficiency of the system should allow its battery to last throughout the lifetime of the underground applications, typically one to three years. The embedded transceivers should be sufficiently compact to fit in a typical borehole, which is 5 to 10 cm in diameter.

In the past 50 years, several attempts toward wireless communication through-soil, connecting underground sensor networks using electromagnetic waves (EM), have been made. A maximum communication range of 130 m was achieved via a system that used low-frequency magnetic dipole radiation, but which required expensive superconducting quantum interference devices as receivers which would require continuous cooling with liquid nitrogen and hence impractical for permanent accesses [2]. Other attempts achieved much shorter ranges and required large antennas, shallow burial depths and were extremely sensitive to the water content of the soil [3]. Magnetic coils were used to generate near-field magnetic induction, but the communication range was limited to less than 10 m without installation of relays [4]. The range and burial-depth limitations of systems are fundamentally due to the inherent extreme path losses of electromagnetic waves in soil compared to vacuum and air; attenuation coefficients on the order of hundreds of dB/m were recorded [3] for 300–700 MHz frequency bands.

Animals have preceded humans in practical and successful communication in water and soil, by employing mechanical rather than electromagnetic waves. Some submarine mammals communicate through water sometimes over thousands of kilometers, while many animals and insects were found to be communicating through-soil, yet over much shorter ranges. Elephants, well equipped to detect seismic cues through either bone conduction or somatosensory reception, produce long repeated seismic pulses by thumping the ground to communicate with each other over long distances [5]. It is conservatively estimated that at least 150,000 insect species also use substrate-borne

vibrations for communications [6]. Inspired by animals, human attempts to communicate through water via ultrasonic waves start to overcome challenges characterized by fast-fading nature induced from the large Doppler and delay spreads. Current state-of-the-art algorithms enable communicating at data rates in excess of 1 Mb/s over 100 m ranges and up to 400 Mb/s over cm-scale distances [7].

Similar advances in underground wireless communications have yet to materialize. One of the few attempts to employ mechanical waves in underground communications was performed decades ago, by inducing low-frequency, high-duration seismic signals via surface-mounted thumpers, that were then detected hundreds of meters away from the sources [8], which inspired the development of some seismic communication schemes, mostly targeting the remote switching of perforating drills [9, 10]. However, this attempt was limited to the transmission of harmonic signals of periods longer than 0.5s, for which a simple communication scheme, such as on-off keying (OOK), may work but would yield extremely low data rates (< 2b/s). Furthermore, the transmitting sources used were surface-mounted, making this system only capable of uni-directional downlink applications from an above-ground base station to underground devices; they are not suitable for Internet of underground things applications, which requires bidirectional connections among fully embedded underground sensors. Additionally, the size of these instruments limits their utility, having pistons larger than 30 cm in diameter.

In this article, we propose the first practical implementation of a reliable wireless through-soil data communication system, simultaneously satisfying requirements for compact size (5–10 cm in diameter), good ranges (up to 50 meters), and low cost installation (due to the utilization of off-the-shelf acoustic sources), making it suitable for underground sensor networks.

## Soil Acoustic Channel Characteristics

Transferring the progress achieved in underwater communications to the underground requires identifying the soil acoustic channel characteristics. While water only admits pressure (primary) waves, soil, a multi-phase material consisting of both solid and liquid components, can simultaneously exhibit both kinds of body waves: pressure and shear (secondary) waves. In addition, the interaction of body waves with superficial layers produces Rayleigh and Love waves [11].

Mechanical waves propagating through-soil attenuate due to geometric and material damping. Geometric damping depends on the type and location of the source of the waves while material damping depends on the material properties and the wave amplitude. Scattering, frictional losses due to grain-to-grain contacts, and viscous losses due to the relative motion between the pore fluid and the sediment frame, are the mechanisms that account for most soil material damping [12]. Energy conversion between different waves and multiple interbed reflections can also introduce significant attenuation [5]. Material damping depends on a host of factors, including plasticity, strain amplitude, effective means stress, void ratio, loading cycles, degree of saturation and thixotropic effects [13]. Theoretical [11] models, laboratory

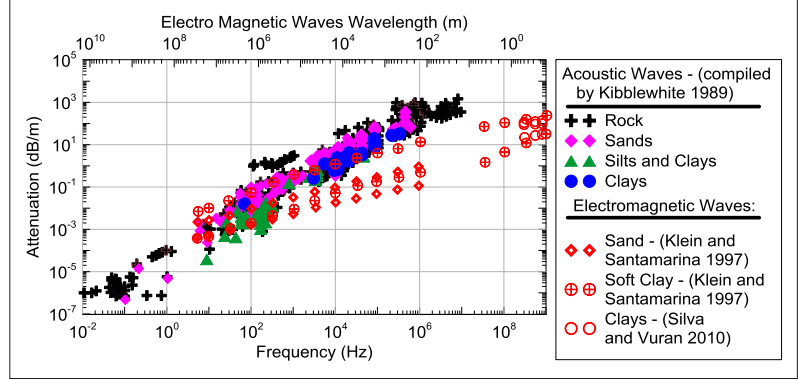


FIGURE 1. Soils attenuation measurements of acoustic and electromagnetic waves.

[14] and field tests [13] show that the geometric damping are represented in loss terms proportional to the inverse square in distance, and the material damping is exponential to frequency and distance. The resulting acoustic path gain over frequencies  $f$  and the path distance  $d$  for a single propagating mode can be written as

$$H(f, d) \propto \frac{1}{d^2} e^{-\alpha 2\pi f d} e^{j 2\pi f d / c}, \quad (1)$$

where  $c$  is the speed of sound in soil with a given configuration and the path arrival time  $d/c$  invokes the phase shift of  $2\pi f d / c$ . The geometric loss of  $d^2$  corresponds to spherical spreading and can be absorbed into the exponential material loss term for long distances; in general, this term can be rewritten as  $d^\gamma$  where  $1 \leq \gamma \leq 3$ . The loss from the material damping can be represented by an attenuation coefficient  $\alpha$ , which has units of  $\text{dBm}^{-1}\text{Hz}^{-1}$ . As explained above, the velocity and loss terms can be determined from various physical parameters of the soil, such as soil plasticity, grain size, and composition. Water content can dramatically increase the material damping loss, even for the same soil type up to tens of  $\text{dBm}^{-1}\text{Hz}^{-1}$  [14]. Some measurements of acoustic attenuation coefficients [13, 15] for various soils are illustrated in Fig. 1 with their electromagnetic counterparts [3].

Soil is typically inhomogeneous with irregular boundaries and varying characteristics; hence, longitudinal and shear waves induced by embedded acoustic sources in surrounding soil follow various paths as shown in Fig. 2a, illustrating a sample stratigraphy from an urban area of San Francisco. Refractions and reflections from layers cause multi-path propagation, and the resulting channel frequency response can be represented by the following equation:

$$H(f) \propto \sum_{i=1}^M k_i e^{-\alpha_i 2\pi f d_i} e^{j 2\pi f d_i / c_i}, \quad (2)$$

where  $k_i$  is a constant complex gain, and  $\alpha_i$ ,  $d_i$  and  $c_i$  each denotes the attenuation coefficient, path distances and the propagation speed of the traveling mode along the  $i^{\text{th}}$  of  $M$  paths. As can be seen from Eq. 2, multimodal and multipath propagation often result in large transmission delay spreads. Even without multi-path effects, the frequency-dependent attenuation in Eq. 1 may result in delay spreads on the order of hundreds of milliseconds

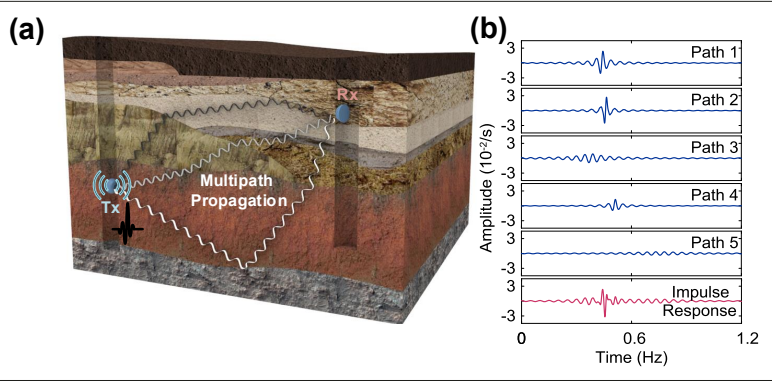


FIGURE 2. Schematic of multipath propagation of acoustic waves in a complex underground stratigraphy; b) Sample resolved impulses of individual propagation paths from a 25m-range measurement taken using a 250W speaker with a 5s-long chirp signal from 20 to 100Hz. All added propagation paths compose the resulting impulse response estimates with a delay spread of 500 ms.

[14]. Figure 2b, for example, illustrates impulse responses along different propagation paths, as estimated from some of our field measurements. Taken together, these phenomena dramatically limit the bandwidth available for reliable wireless through-soil communication.

Operating at sufficiently low frequencies, characterized by lower attenuation and dispersion levels, is possible using acoustic transducers, but impractical using electromagnetic transducers owing to the impractically long antennas required for transmission. This justifies using acoustic waves rather than electromagnetic waves as data carriers, although Fig. 1 shows lower attenuation levels for frequencies above 100 Hz. Based on Fig. 1, a 10-kHz electromagnetic wave propagating in moist sand, would benefit from a relatively low attenuation of 0.1 dB/m, but would require a quarter wavelength antenna size of at least 3.75 km. Acoustic frequencies below 100 Hz can benefit from the same level of attenuation with sources smaller than 30 cm in size. These frequencies, although relatively low and hence can support only low data-transmission bandwidth, are suitable for numerous underground applications requiring data rates below 100 b/s, in which transceiver size, ease and feasibility of deployment and robustness are more critical than achievable data bandwidth.

### SYSTEM ARCHITECTURE

Overcoming challenges due to multi-mode and multi-path nature with the frequency dependent path loss, here we propose a through-soil node-to-node communication system suitable for underground sensor networks. A simple but efficient sparse decision feedback equalization (DFE) technique is proposed to compensate inter-symbol interference (ISI), leveraging the physical model of soil acoustic channels described in the previous section.

### CODING/MODULATION SCHEMES

In underwater acoustic communications, both single carrier modulation techniques, such as M-ary phase shift keying (M-PSK) and quadrature amplitude modulation (M-QAM), and multi-carrier methods, including frequency shift keying (FSK) and orthogonal frequency-division modulation

(OFDM), are broadly used for modulation. However, in soil acoustic channel, because of the bandwidth limitation remarked in the previous section, multi-carrier schemes are not considered practical. Therefore, low order single-carrier linear constellation schemes, such as on-off keying (OOK), and quadrature phase shift keying (QPSK), are considered in the proposed system. Also, a binary message, which includes the information of underground sensors, is encoded using forward error correction designed specifically for the application; 2/3 rates systematic convolutional codes were adopted here, but the coding rate can be adapted with application ranges. The encoded data is then combined via XOR to a pseudo-random whitening code to protect the data from time-correlated or periodic noises that are common for acoustic channels in urban areas.

### FRAME STRUCTURE

As can be seen in Fig. 3b, a communication packet is generated comprising a preamble sequence for packet detection and synchronization, a training sequence for channel estimation and equalizer tracking, and load data. Between the preamble and data sequence, a guard interval is inserted to avoid the corruption from delay spreads of the preamble sequences. Also, after data packets of up to 15,000 bits, of which the first 1,000 bits were used for training, are sent, the system undergoes a rest phase to account for heating issues of transducers. For the preamble waveform, either a 13-bit Barker sequence or linear frequency modulation (LFM) chirp signal can be used for packet detection, that is, applying a matched filter to the preamble waveform at the receiver, the packet boundary can be determined by the peak. Furthermore, the impulse-like autocorrelation of the preamble, which is designed to minimize off-peak autocorrelation, makes the matched filter output a coarse estimate of the channel impulse response that can be used for initializing clock synchronization and equalizer parameters.

### SPARSE DFE DESIGN VIA MULTIPATH RESOLUTION

Equalizers are indispensable elements of modern digital transmission systems used to maximize throughput over a dispersive channel by compensating ISI. Decision feedback equalizers (DFE) outperform linear methods, in terms of their ability to mitigate ISI due to multi-path propagation. These nonlinear processors combine a forward-filtered version of the received signal and an estimate of interference through feedback-filtered nonlinear symbol estimates from previous timesteps. Longer delay spreads typically require longer feedforward and feedback filters, which increase computational complexity as well as the deleterious effects of error propagation [16]. In this work, equalizer parameters are determined by leveraging a physical model of the soil channel described in Eq. 2. Because this model can be interpreted as a linear combination of damped complex exponential, which can be easily decomposed by Prony's or matrix pencil methods [17], the impulse response estimated from the preamble sequence also can be decomposed into a series of single-path impulses having different arrival times. Since the DFE is used to compensate for multipath, it is effective to only update feedback filter taps at locations in

the neighborhood of the  $M$  arrival times  $T_i = d_i/c$ , instead of updating all locations within the entire delay spread, as illustrated in Fig. 3c. This reduces the complexity of the equalizer compared to the conventional approach of parameterizing the entire delay spread of the channel. As can be seen in Fig. 2b, a typical through-soil impulse response comprising five paths with a line-of-sight distance of 25 m can have a delay spread longer than 500 ms. If the symbol rate is 100 sps, a conventional finite impulse response (FIR) model would require 50 taps, while a path-specific model (2) requires only 15 parameters to represent the channel. In Table 1, such estimated parameters for the sample 25m-range impulse response measurement in Fig. 2b are summarized.

## CLOCK SYNCHRONIZATION

Although soil acoustic channels do not typically suffer from motion-induced Doppler spreads, their performance can be critically degraded with the existence of carrier frequency offsets (CFO) due to the Tx/Rx clock synchronization failure. In our system, simple phase tracking techniques, such as linear phase-locked loop (PLL), can be adopted. At first, the phase offset value can be initialized by using the impulse response values estimated from the preamble sequence. Then, phase offsets can be computed symbol by symbol in the equalizer, as illustrated in Fig. 3a, and are fed back into the demodulation stage, compensating for remaining CFO.

The entire data transmission architecture is depicted in Fig. 3 as follows. First, a channel coded message is XOR-combined with the spreading code  $s$ , and divided in parallel through a demultiplexer (demux) to in-phase and quadrature-phase components. Each component is pulse shaped by low-pass filters (LPF), modulated onto the carrier frequency  $F_c$ , and transmitted to soil layers via off-the-shelf electroacoustic devices, such as tactile speakers. After traveling through-soil, the acoustic signal is collected electrically via a hydrophone/geophone. The received signal is demodulated into the complex baseband and sampled at half of the symbol period,  $T/2$ . Symbol decisions  $\hat{d}$  are made by the decision feedback equalizer described in the bottom of Fig. 3a; parameters of equalizers are adaptively updated by the recursive least squares (RLS) algorithm, where errors between equalizer outputs and known symbols are used for the RLS input  $e$  during training mode, while past decisions are used during decision-directed mode.

## TESTING

The communication system developed here can be adjusted to suit different applications with varying data rates, ranges and power requirements. For example, through-soil acoustic data links can be implemented for a buried pipeline monitoring system, potentially supporting data rates of hundreds of bps for short-range links to detect and report leakages in real-time. However, underground infrastructure monitoring sensors at construction sites might only require a few bps in data rates over communication distances of up to 50 meters. To show the viability and versatility of the approach, two sets of experiments were conducted: laboratory experiments simulating short-range high-data-rate applications and field experiments

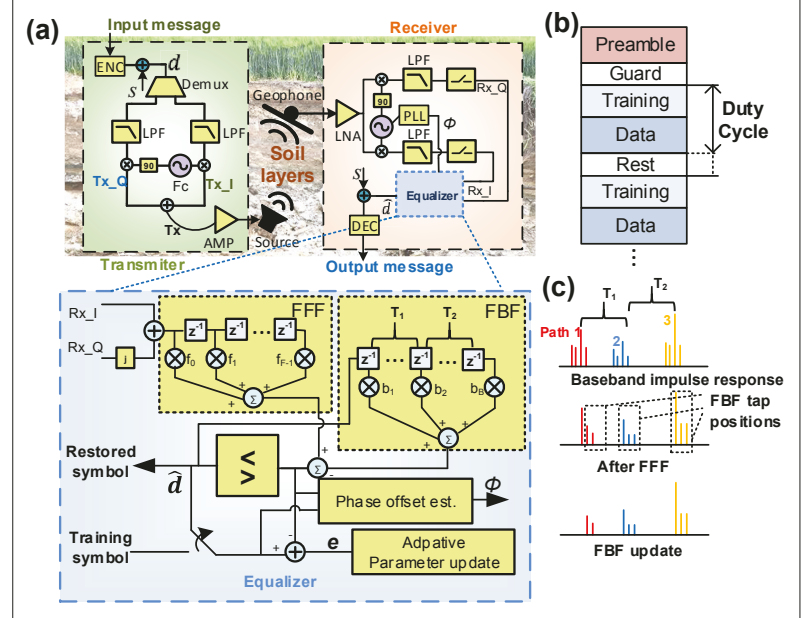


FIGURE 3. a) Schematic of the communication system using off-the-shelf speakers and hydrophones; b) the corresponding frame structure of the transmitted waveform; c) design method for the sparse DFE, given a multi-path resolved impulse response.

Path index $i$	$k_i (10^{-3})$	$2\pi\alpha_i d_i (\text{dB/Hz})$	$c_i/d_i (\text{ms})$
1	$0.8936 - 0.2410i$	0.0991	438.9
2	$-0.6334 - 0.0890i$	0.0525	459.1
3	$0.9016 + 0.8177i$	0.4018	376.6
4	$-0.3152 - 0.4303i$	0.1143	509.7
5	$-0.1946 + 0.9777i$	0.9361	790.8

TABLE I. Estimated parameters of a path-specific model (2) for the sample 25m impulse response measurement in Fig. 2b.

simulating long-range low-data-rate applications.

Laboratory tests were designed to check the limit on achievable data-rates for shorter distances less than a meter with different parameters, such as coupling materials and saturation levels. A  $2 \times 0.5 \times 0.5$  m sized metal trough, equipped with sound dampening wooden plates attached to the inner walls to prevent the sound reflection, and filled with uniform clean fine sand (SP), was used to simulate a shallow depth soil channel in the chamber. In quiet lab conditions, electrical noises in data collecting device dominate to the acoustic counterpart, resulting averagely  $-110$  dBm/Hz noise floor on acoustic frequency ranges.

Field tests were designed to target maximum achievable ranges, while experiencing natural soil conditions typically encountered in construction or agricultural sites. They were conducted at a field area south of Champaign, IL, whose top soil layer, of approximately 1 m thickness, is characterized as organic clay ( $w_0 = 16$ ,  $LL = 57$ ,  $PI = 32$ ), while the layer below consisted of organic silt ( $w_0 = 26$ ,  $LL = 40$ ,  $PI = 17$ ). Acoustic transducers and receivers were installed in boreholes of 20 cm in diameter at depths ranging between 30 and 150 cm. Measurements were conducted by changing node distances for 15, 25, 35, and 50 m distances. To maintain good contact between soil and transceivers, clean fine sand was poured and compacted in boreholes

after installation of transceivers. In Fig. 4a, photos of both the laboratory setting and the field site are depicted. In this area, averagely  $-105$  to  $-95$  dBm/Hz noise was recorded at the measuring device upon different environmental conditions including strength of surface wind or number of cars driving near the place.

Before transmitting digitally modulated signals, frequency responses, at different frequencies, were measured by sweeping probe harmonic signals through the channel to determine optimal frequency ranges for each transmissions; only acoustic frequencies for which the received signals were

above the noise floor were chosen for data transmission. For example, in Fig. 4b, the estimated frequency response is shown for two channels, one in the laboratory with a range of 30 cm, and another in the field with a range of 25 m. In the laboratory, characterized by its short target range, a frequency range of 500–1500 Hz was adopted, based on its frequency response illustrated in the first row of Fig. 4b. In the field, where ranges around 25 meters were targeted, the electrical noise floor was at  $-104.6$  dBm/Hz, and only the frequency range whose response was above this floor was used; that is, 20–80 Hz was chosen as the target frequency range as illustrated in the second row of Fig. 4b.

Following the frequency sweep measurements, a set of data transmission tests were conducted to prove the viability of our proposed system. As remarked earlier, two different sets of benchmark waveforms were generated; one is a family of higher data rate QPSK-modulated signals for laboratory testing with a carrier frequency of 1 kHz, and the other has subsonic to seismic frequency ranges, resulting in lower-data-rate signals suitable for longer distance field testing. Data restoration of these benchmark transmissions after equalization is illustrated in the constellations in Fig. 4b. In the first row of the figure, it is shown that data can be reliably restored with extremely low bit error rates ( $\leq 1E-04$ ) from a 2 kb/s QPSK signal transmitted from the 30 W source 30 cm away from the receiver, which shows the viability of the system for higher data rate applications. This result corresponds to tests in dry sands; for the water saturated case, when the path loss for the same distance can be larger than that of dry sand by more than 10 dB, data rates had to be adjusted to half, to successfully restore 1 kb/s signals. Also, for 60 cm ranges, 1 kb/s and 500 bps data rates were achieved without bit errors for dry and water saturated conditions. The second row of Fig. 4b shows the successful restoration of data in the field with 15 dB SNR margin at the equalizer output, where a 20 bps QPSK signal with a 30 Hz carrier frequency was transmitted from the 250 W source over a 25 m range, illustrating the viability of the system for longer distance applications.

In summary, key measurement results covering achieved ranges, data rates, and energy per transmitted bit (bits/Joule) are depicted in Fig. 4c. In shorter-distance laboratory settings, up to 2 kb/s and 1 kb/s data rates for 30 cm distances were achieved through dry sand and water-saturated sand, respectively. Reliable communication ( $BER < 1E-04$ ) with 2 bps data rates was achieved at a range of 50 m in outdoor field experiments, while at ranges of up to 35 m, 20 bps data rates were achieved.

## SMALL-SIZE POWER-EFFICIENT SOURCE DESIGN

To be feasibly employed in underground applications, acoustic sources should be capable of delivering frequencies suitable for the channel characteristics and target data rate; small enough to fit within typical boreholes (2 to 4 inches in diameter); power-efficient, water-tight, impedance-matched to the soil; capable of delivering sufficient acoustic power over a practical range; and compatible with modulation. Attenuation measurements from the literature and from our channel characterization tests confirmed that

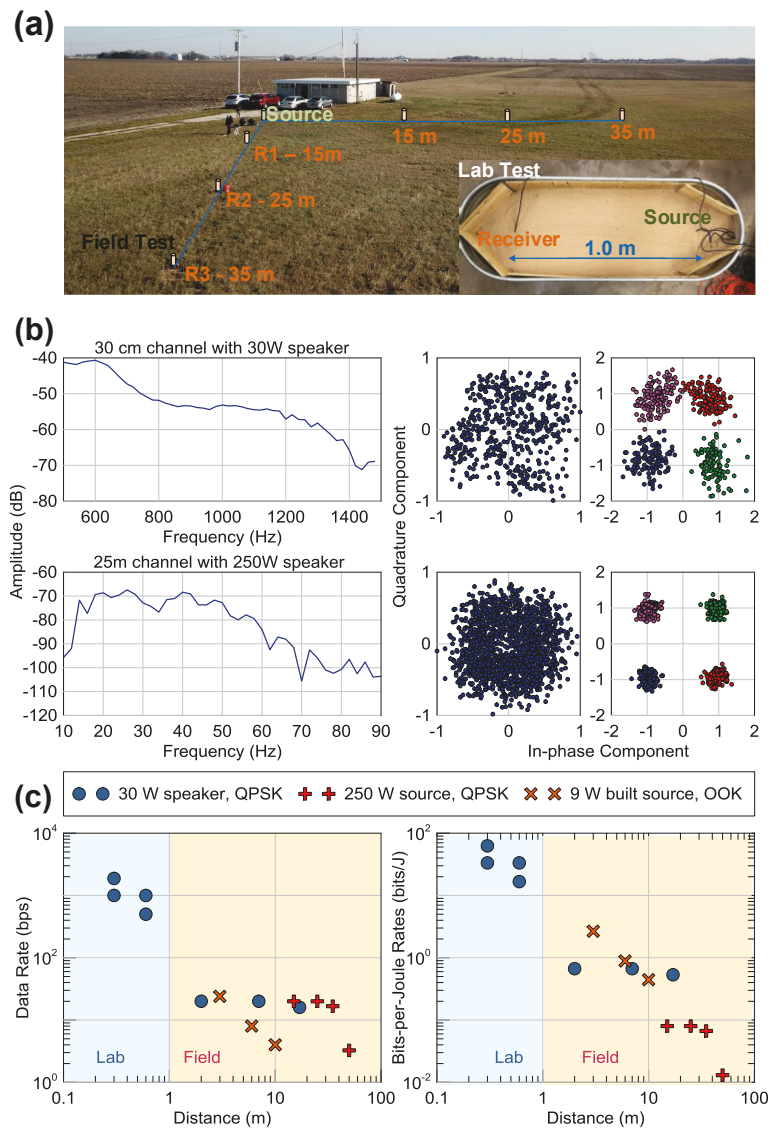


**FIGURE 4.** a) Photos showing the experimental data transmission setup for through-soil acoustic communication and their transmission results; b) Channel response (left), constellation diagrams of received symbols before (center) and after (right) the equalization are shown for soil electroacoustic channels using the 30 W speaker tested in the laboratory over a range of 30 cm (top) and using 250 W speaker deployed at 50 cm depth at the field area shown in (a) over a range of 25 m (bottom); resulting constellations are from QPSK modulated probe signals with 1-kHz center frequency and 1-kHz symbol rate in the laboratory (top right), 30-Hz center frequency and 10-Hz symbol rate at the field area (bottom right) respectively; c) Performance of soil acoustic communication using commercial speakers and new source design employing a VCA motor: Data rates vs. distance (left), and bits / joule vs. distance (right).

lower-frequency waves suffer less attenuation. Although lower frequencies imply lower available bandwidth and therefore lower data rates, they increase the range of transmission, which is currently the major limitation for non-acoustic (e.g., electromagnetic) systems. Based on our measurements, frequencies ranging between 10 and 40 Hz attained ranges and data rates that would be of interest for a wide range of potential applications. Common loud speakers are unable to effectively deliver frequencies in this range, and speakers that can deliver such frequencies are necessarily characterized by larger dimensions that exceed typical borehole diameters of two to four inches. Larger speakers also yield greater contact areas with the soil over which power is distributed, hence reducing stress wave amplitudes. They also suffer from acoustic coupling issues, since their short strokes are incapable of ensuring contact with the often poorly-compacted soil, especially since excellent compaction around embedded sources is hard to achieve in small-sized boreholes. This coupling issue can result in severe energy losses even before the signal is transmitted into the soil. Short strokes prevent speakers from accumulating high kinematic energy that is converted to high amplitude stress waves. While common loud speakers are designed to match air impedances and underwater speakers are designed to match those of water, there are no commercial speakers designed to match the impedance of soil, which is characterized by high spatial variability. Such limitations of available speakers, which were reflected through our own and previous authors' laboratory and field communication test results, suggested the need for designing a new source. The authors developed a design that employs a voice coil actuator (VCA) characterized by a maximum stroke of 19 mm and a maximum continuous power of 18 W. The source used two controllers, powered by four Li-ion batteries and cased in plexiglass. A 12 mm  $\times$  12 mm plexiglass cap was attached to the actuator head, thus reducing the area of contact with soil and increasing the amplitude of the stress wave. The source was sufficiently small to fit into a 4-in-diameter borehole.

A power-efficient on-off keyed modulation scheme was employed; a logical "1" is represented by a single or multiple mechanical impulses generated by hammering the motor head against soil, as described in Fig. 5, while a logical "0" is represented by the absence of any impulse. The modulation order can be modified by changing the number and location of impulses, while the period of each impulse is fixed by design, that is, in our design, this period was set at 1/24s. The motor operates in 9W average power consumption, assuming equivalent priors for "on" and "off" states. An Arduino Uno 3 microcontroller board was chosen to deliver the electric control signal to the motor controller. The receiver structure, illustrated in Fig. 5, is similar to that used for commercial speakers, but differs in two perspectives. First, the scheme only assumes real-valued symbols, while the system described in Fig. 3a deals with symbols modulated over a complex domain. Second, symbol timing jitter can be substantially larger in this type of design due to variations in mechanical operation of the motor. Therefore, to ensure reliable operation of PLL, a

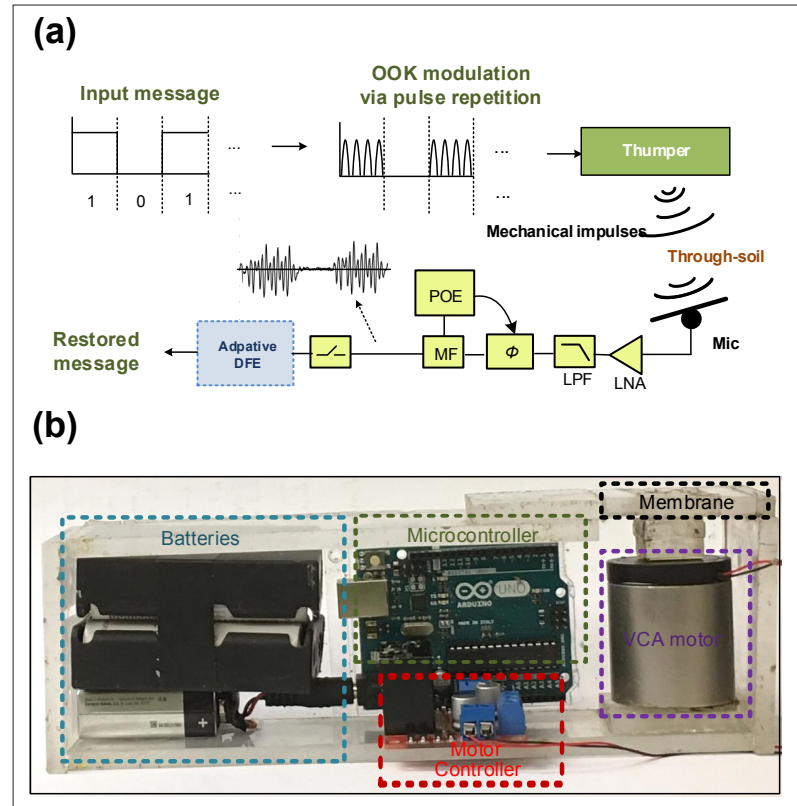


FIGURE 5. a) Schematic of the communication system with the proposed source using OOK modulation based on repetitive pulse generation; b) Photo of the built small source.

pilot symbol on each packet composed of 100 symbols was added.

As a result, 24 b/s data rate was achieved over distances less than 5m with bit error rates less than  $1E-04$ . This was achieved by modulating logical "1" symbols with a single mechanical stroke. For distances greater than 5m, bit errors occur more frequently due to the larger path loss and multipath scattering. This is described in Fig. 6a, where received data over 10m distance is illustrated in the form of a histogram; before equalization, in which many outputs due to "1" and "0" symbols are overlapped, causing errors in symbol decisions, and even after applying the equalization technique depicted in Fig. 5, a number of bit errors persist. Therefore, forward error correcting codes were adopted to resolve residual errors. For example, when sending data over a range of 10m, a rate 1/6 convolutional code was exploited to encoding for reliable data transmission. Based on this setting, 4 bps rates for ranges up to 10 meters were achieved. Even though these rates are lower than those from the system employing higher-power, off-the-shelf speakers, energy efficiency, which is defined as the amount of information that can be transferred using a Joule of energy, was only 2.7 bits/J for the 5 m channel in this case, compared to a 0.7 bits/J for off-the-shelf speakers, as illustrated in Fig. 4b. If the source is to provide one reading equivalent to 100 bits every day (which is sufficient for a geotechnical piezometer, for example), the current prototype can serve for 45 months before its Li-ion batteries are exhausted. For illustrating the new systems functionality, a 192  $\times$  192 pixels JPEG-encoded image was transmitted through-soil

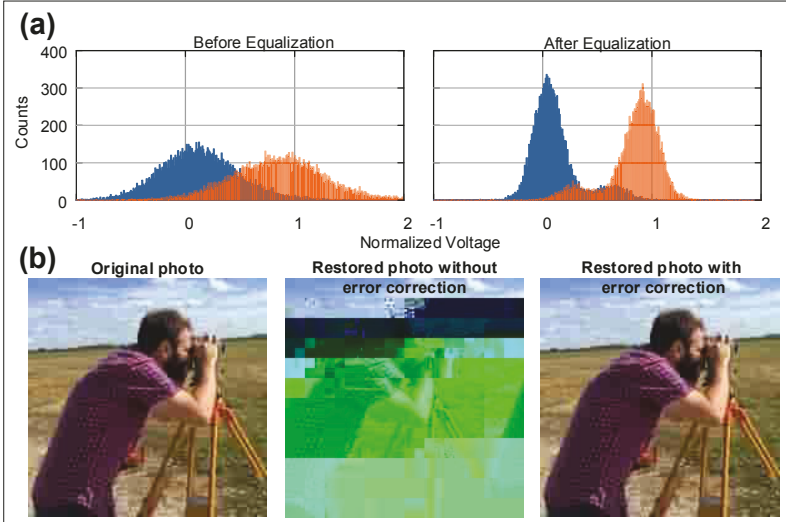


FIGURE 6. Illustration of results of the On-Off keyed system operated with the proposed small source: a) Histograms of restored symbols from 10m data transmission using the small source before (left) and after (right) applying the equalization algorithm; red and blue bins refer logical “0,” and “1” symbols respectively; b) the original photo sent over 10 m in the field area using the built small source (left), the restored image without error correction (center), and the restored image after error correction (right).

using the suggested source. Figure 6b shows the raw restored image sent over a 10-m range in the field. Only 0.17 percent bit errors occurred, and the convolutional code was successful in correcting those errors.

An underground sensor system can benefit from the developed wireless communication system by equipping each embedded sensor with a small acoustic source, as presented in [5]. The current source prototype cost is on the order of a few hundred dollars, but can be greatly reduced with mass-production. Without wire congestion or entanglement, the sensor deployment is much simpler, and more sensors can be deployed within a small-size borehole than for the current wired approach.

## Conclusion

A compact underground wireless acoustic data transmission system capable of communicating data up to 50 meters in range without deploying additional relay nodes was presented. An embedded transmitter, small enough to fit in a typical 4-inch-diameter borehole, was also developed and has the potential to dramatically lower the cost of underground sensor deployment while increasing the safety of monitored structures and agriculture. The architecture of this platform is of low complexity compared to other acoustic communication systems, such as those for underwater environments. Computational loads were substantially reduced as compared with underwater acoustic systems, with complexity reductions arising from sparse multipath modeling, simple phase tracking and no explicit Doppler compensation, since underground soil layers are effectively stationary in time, and modest data requirements, leading to substantially lower operating frequencies.

While the authors proposed a small thumper-source showing a superior energy efficiency, compactness, and suitability for target frequency

ranges, when compared to commercial off-the-shelf speakers, the design can be further optimized in many ways. Exploiting the nonlinearity of the soil layers may enable the design of substantially more directional sources avoiding most geometric losses in propagation. Although only point-to-point communication scenarios were considered in this study, multiple-input-multiple-output (MIMO) techniques can be applied to network scenarios.

## ACKNOWLEDGMENT

The authors would like to thank the National Science Foundation (NSF) and Dr. Richard Fraga for the financial support of this work under grant number NSF CMMI 1643025. The views expressed in this article are those of the authors and do not necessarily represent the views of NSF.1643025.

## REFERENCES

- [1] D. Teal, “Cordless Geo Data-Link,” *GeoTechnical Instrumentation in Practice: Purpose, Performance and Interpretation*, Thomas Telford Publishing, 1990, pp. 617–28.
- [2] J. Vasquez, V. Rodriguez, and D. Reagor, “Underground Wireless Communications Using High-Temperature Superconducting Receivers,” *IEEE Trans. Applied Superconductivity*, vol. 14, 2004, pp. 46–53.
- [3] A. R. Silva and M. C. Vuran, “Communication with Above-Ground Devices in Wireless Underground Sensor Networks: An Empirical Study,” *Proc. 2010 IEEE Int'l. Conf. Commun. (ICC)*, pp. 1–6.
- [4] Z. Sun and I. F. Akyildiz, “Magnetic Induction Communications for Wireless Underground Sensor Networks,” *IEEE Trans. Antennas and Propagation*, vol. 58, 2010, pp. 2426–35.
- [5] O. Baltaji *et al.*, “Through-Soil Wireless Communication System for Embedded Geotechnical Instrumentation,” *American Society of Civil Engineers*, Reston, VA, 2019, pp. 200–08.
- [6] W. Kojima, T. Takanashi, and Y. Ishikawa, “Vibratory Communication in the Soil: Pupal Signals Deter Larval Intrusion in a Group-Living Beetle *Trypoxylus Dichotoma*,” *Behavioral Ecology and Sociobiology*, vol. 66, no. 2, 2012, pp. 171–79.
- [7] T. Riedl and A. Singer, “Towards a Video-Capable Wireless Underwater Modem: Doppler Tolerant Broadband Acoustic Communication,” *Proc. 2014 IEEE Underwater Commun. Networking (UComms)*, 2014, IEEE, pp. 1–5.
- [8] K. Ilkrah and W. Schneider, “Communications via Seismic Waves Employing 80-Hz Resonant Seismic Transducers,” *IEEE Trans. Commun. Technology*, vol. 16, no. 3, 1968, pp. 439–44.
- [9] T. D. Brumleve, M. G. Hicks, and M. O. Jones, “System for Remote Control of Underground Device,” Oct. 21 1975, US Patent 3,914,732.
- [10] J. L. Harmon and W. T. Bell, “Downhole Process Control Method Utilizing Seismic Communication,” June 24 2003, US Patent 6,584,406.
- [11] S. L. Kramer, *Geotechnical Earthquake Engineering*, Prentice-Hall, New Jersey, 1996.
- [12] B. A. Brunson, “A Comparison Between BIOT Model Predictions and Shear Wave Attenuation Measurements in Unconsolidated Laboratory Sediments,” *The Journal of the Acoustical Society of America*, vol. 74, no. S1, 1983, pp. S59–S59.
- [13] M. Vucetic and R. Dobry, “Effect of Soil Plasticity on Cyclic Response,” *J. Geotechnical Engineering*, vol. 117, no. 1, 1991, pp. 89–107.
- [14] M. L. Oelze, W. D. O’Brien, and R. G. Darmody, “Measurement of Attenuation and Speed of Sound in Soils,” *Soil Science Society of America J.*, vol. 66, no. 3, 2002, pp. 788–96.
- [15] K. Klein and J. C. Santamarina, “Methods for Broad-Band Dielectric Permittivity Measurements (Soil-Water Mixtures, 5 Hz to 1.3 GHz),” *Geotechnical Testing J.*, vol. 20, no. 2, 1997, pp. 168–78.
- [16] M. Reuter *et al.*, “Mitigating Error Propagation Effects in a Decision Feedback Equalizer,” *IEEE Trans. Commun.*, vol. 49, no. 11, 2001, pp. 2028–41.
- [17] R. C. Qiu and I.-T. Lu, “Multipath Resolving with Frequency Dependence for Wide-Band Wireless Channel Modeling,” *IEEE Trans. Vehicular Technology*, vol. 48, no. 1, 1999, pp. 273–85.

## BIOGRAPHIES

SIJUNG YANG received the B.S. degree in electrical engineering from Seoul National University, Seoul, South Korea in 2014, and the M.S. degree in electrical engineering from the University of Illinois at Urbana-Champaign, Urbana, IL, USA in 2017, where he is currently working toward the Ph.D. degree in electrical engineering. His research interests are the fundamental limits and optimal implementations of seismic/acoustic/ultrasonic communication systems, and energy efficient communication system design, which targets Internet of things networks deployed on urban areas.

OMAR BALTAJI received his B.E. from Beirut Arab University (2013), his M.S. from the University of Illinois at Urbana-Champaign (2015), and he is currently pursuing a Ph.D. in civil engineering at the University of Illinois at Urbana-Champaign. His research interests include deep excavations, instrumentation systems, geotechnical earthquake engineering, numerical and constitutive modeling.

ANDREW C. SINGER received the S.B., S.M., and Ph.D. degrees, all in electrical engineering and computer science, from the Massachusetts Institute of Technology. Since 1998, he has been on the faculty of the Department of Electrical and Computer Engineering at the University of Illinois at Urbana-Champaign, where he currently holds a Fox Family Endowed Professorship in the Electrical and Computer Engineering Department and serves as Associate Dean for Innovation and Entrepreneurship in the College of Engineering. During the academic year 1996, he was a postdoctoral research affiliate in the Research Laboratory of Electronics at MIT. From 1996 to 1998, he was a research scientist at Sanders, A Lockheed Martin Company in Manchester, New Hampshire. He was co-founder of Intersymbol Communi-

cations (now a subsidiary of Finisar) and of OceanComm, Inc., a provider of Mb/s underwater acoustic modem technology. In 2006, he received the *IEEE Journal of Solid State Circuits* Best Paper Award and in 2008 he received the *IEEE Signal Processing Magazine* Award. In 2009, he was elected a Fellow of the IEEE "for contributions to signal processing techniques for digital communication," and in 2014, he was named a Distinguished Lecturer of the IEEE Signal Processing Society.

YOUSSEF M. A. HASHASH holds a B.S. (1987), an M.S. (1988) and a Ph.D. (1992) in civil engineering from the Massachusetts Institute of Technology. He began his career with the PB/MK TEAM in Dallas on the Superconducting Super Collider Project. In 1994 he joined Parsons Brinckerhoff in San Francisco and worked on a number of underground construction projects in the U.S. and Canada, including the Boston Central Artery/Tunnel project. Professor Hashash joined the faculty of the Department of Civil and Environmental Engineering at the University of Illinois at Urbana-Champaign in 1998. He taught courses in Geotechnical Engineering, Numerical Modeling in Geomechanics, Geotechnical Earthquake Engineering, Tunneling in Soil and Rock, and Excavation and Support Systems. His research focus includes deep excavations in urban areas, earthquake engineering, continuum and discrete element modeling and soil-structure interaction. He also works on geotechnical engineering applications of visualization, augmented reality, imaging and drone technologies in. He has published over 100 journal articles and is a co-inventor on four patents. His research group developed the software program DEEPSOIL that is used worldwide for evaluation of soil response to earthquake shaking. He is a Fellow of the American Society of Civil Engineers (ASCE) and has received a number of teaching, university and professional awards including the Presidential Early Career Award for Scientists and Engineers and the ASCE 2014 Peck medal.